
Proceedings Paper:
Shahbazi, Fatemeh, Esfahani, Mohammad Nasr orcid.org/0000-0002-6973-2205, Jabbari, Masoud et al. (1 more author) (2022) A Molecular Dynamics Model for Biomedical Sensor Evaluation:Nanoscale Numerical Simulation of an Aluminum-Based Biosensor. In: 44th Annual International Conference of the IEEE Engineering in Medicine and Biology Society, EMBC 2022. 44th Annual International Conference of the IEEE Engineering in Medicine and Biology Society, EMBC 2022, 11-15 Jul 2022 Proceedings of the Annual International Conference of the IEEE Engineering in Medicine and Biology Society, EMBS. Institute of Electrical and Electronics Engineers Inc., GBR, pp. 613-616.

https://doi.org/10.1109/EMBC48229.2022.9871498

2022 44th Annual International Conference of
the IEEE Engineering in Medicine & Biology Society (EMBC)
Scottish Event Campus, Glasgow, UK, July 11-15, 2022

2022 44th Annual International Conference of the IEEE Engineering in Medicine & Biology Society (EMBC) | 978-1-7281-2782-8/22/$31.00 ©2022 IEEE | DOI: 10.1109/EMBC48229.2022.9871498

A Molecular Dynamics Model for Biomedical Sensor Evaluation: Nanoscale Numerical Simulation of an Aluminum-Based Biosensor *

Fatemeh Shahbazi, Mohammad Nasr Esfahani, Masoud Jabbari, Amir Keshmiri.

***Abstract*— Metallic nanostructured-based biosensors provide label-free, multiplexed, and real-time detections of chemical and biological targets. Aluminum-based biosensors are favored in this category, due to their enhanced stability and profitability. Despite the recent advances in nanotechnology and the significant improvement in development of these biosensors, some deficiencies restrict their utilization. Hence a detailed insight into their behavior in different conditions would be crucial, which can be achieved with nanoscale numerical simulation. With this aim, an Aluminum-based biosensor is chosen to be analyzed with the help of all-atom molecular dynamics model (AA-MD), using large-scale atomic/molecular massively parallel simulator (LAMMPS). The surface properties and adsorption process through different flow conditions and various concentration of the target, are investigated in this study. In the future work, the results of this study will be used for developing a predictive model for surface properties of the biosensor.**

***Clinical Relevance*— The role of biosensors in clinical applications and early diagnosis is evident. This work provides a model for predicting the binding behavior of the target molecules on the biosensor surface in different conditions. Results demonstrate an increase in the adsorption of ethanol on the biosensor surface of 7% up to 80% with changing the velocity from $0.001\,\mathrm{m/s}$ to $1\,\mathrm{m/s}$ Although for cases with higher concentration, this trend becomes complicated, necessitating the implementation of machine learning models in the future works.**

I. Introduction

The properties of materials undergo remarkable changes when they are processed to the nanometre scale. Chemical, electrical, mechanical, optical, thermal, magnetic, and acoustic properties are affected through this change. Hence, nanomaterials, including Nano metals, graphene, nanowires, nanotubes, and nanoparticles, have attracted a great attention in recent years[1], especially in the biological applications [2–4], diagnosis [5], wearable and flexible devices [6,7]. Aluminium-based biosensors are cost-effective material and relatively stable. Although oxidation and material degradation are their challenges, which can be addressed by passivation treatments such as depositing a dielectric film[25]

Ethanol is an organic compound, which is a simple alcohol. It has crucial roles in medical applications, synthesis of organic compounds and indicating the level of microbiome[8,9]. The biosensor studies on ethanol adsorption are mainly experimental and only a few attempts have been done to study the details of interaction of ethanol with aluminium surface in molecular level [10–13]. In previous attempts, molecular interaction of the solvent and surface are studied without considering the fluid flow behaviour of the solvent[10].

In the current work, the mechanism of ethanol adsorption on an aluminum-based biosensor surface is studied with the help of molecular dynamics (MD) simulations (Figure 1). Sixteen cases have been studied in this work. The effect of the flow rate and concentration on binding kinetics, adsorption, and biosensor performance is studied.

II. Methodology

In the present study, a nanoscale model has been developed using atomic simulations for predicting the binding and surface properties of an Aluminium-based biosensor. In the first step, the configuration of the target molecule is recognized, and the most stable molecule structure is obtained from previous density functional theory (DFT)[14] studies. This study does not include the water molecules. The numerical setup, sensor surface and ethanol molecules are presented in Figure 1. The periodic boundary is used for the x and y directions and fixed boundary for the z direction.

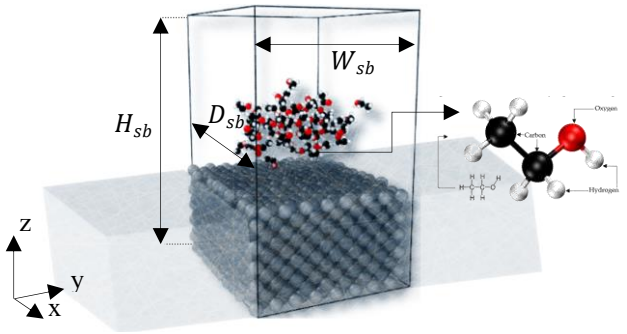

Figure 1. A nanoscale model developed based on atomic simulations, representing the Aluminum slab as a sensor, boundaries and CPK (Corey, Pauling, Koltun) presentation of Ethanol.

In the next step, the Aluminium slab is fixed at the bottom of the simulation box, while Ethanol molecules flow on top of

*Research supported by the department of mechanical, aerospace, and civil engineering, University of Manchester.

F. S., Author, is with the department of mechanical, aerospace, and civil engineering, University of Manchester, Manchester, United Kingdom M17DN (phone: 755-189-0531; e-mail: Fatemeh.shahbazi@manchester.ac.uk).

M. N. E. Author is with the department of Electronics, University of York, York, United Kingdom (e-mail: mohammad.nasresfahani@york.ac.uk).

M. J. Author is with the department of mechanical, aerospace and civil engineering, University of Manchester, Manchester, United Kingdom M17DN (e-mail: m.jabbari@manchester.ac.uk).

A. K. Author is with the department of mechanical, aerospace and civil engineering, University of Manchester, Manchester, United Kingdom M17DN (e-mail: a.keshmiri@manchester.ac.uk).

the aluminium surface (Figure 1). Table I provides the details of the dimensions, concentrations, and flow conditions.

Then reaction force field is used to simulate the interaction between atoms. The most updated version of reactive force field (ReaxFF) alongside with the large-scale atomic/molecular massively parallel simulator (LAMMPS)[15] are used in the current work. A force field is a set of parameters which are used to calculate the potential energy of the simulated atoms. For an atomistic force field, one needs parameters for every type of atom. The parameters for this study are validated with the quantum mechanical calculations in the previous literature[14]. This force field would include parameters for every possible interaction between atoms (bond, angle, dihedral, VSW and columbic) in the simulation.

Reactive force field provides valid quantitative description of reaction kinetics. Liu et al. has tested this capability for Aluminium (Al) and hydrocarbon radials, hydroxyl an ethanol molecule [16]. They carried out this verification by implying QM methods and comparing the results to the previous Reactive force field results[17]. Reactive force field is developed by Van Duin et al [18]. It is a universal force field that implements distance-dependent bond-order function (Equation (1)) to represent the contribution of chemical bonding to the potential energy. In reactive force field, the overall system energy is described as Equation (1).

$$\begin{aligned} E_{system} \\ = E_{bond} + E_{lp} + E_{over} + E_{under} + E_{val} + E_{pen} \\ + E_{coa} + E_{C_2} + E_{triple} + E_{tors} + E_{conj} + E_{H-bond} \\ + E_{vdWaals} + E_{Coulomb} \end{aligned} \quad (1)$$

where E_{bond} is the bond energy, which is determined from the bond order. In this method the bond orders (BO_{ij}) between atoms are estimated from their interatomic distances [19]. E_{lp} presents the lone pair (non-bonding pair) energy.

TABLE I. THE DETAILS OF THE GEOMETRY AND CONDITIONS OF THE MOLECULAR DYNAMICS SIMULATION

	Details of the geometry and MD simulation		
	Sign	***Description***	***Value***
1	H_{sb}	Height of the simulation box (m)	4.2×10^{-9}
2	W_{sb}	Width of the simulation box (m)	3.5×10^{-9}
3	D_{sb}	Depth of the simulation box (m)	3.4×10^{-9}
4	t_{Al}	Thickness of the Aluminum slab (m)	1.65×10^{-9}
5	To_E	Stopping tolerance for energy (-)	10^{-10}
6	To_F	Stopping tolerance for force (Kcal/ mole − Angstroms)	10^{-10}
7	V_{tm}	Velocity of the targeted molecules (m/s)	10
8	T_{md}	The environment temperature (K)	300

Once the total bond order, associated with a particular atom, exceeds its specific amount, it causes a lone pair to gradually brake up. This process is complemented with an energy penalty, which is called the lone pair energyE_{over} and E_{under} are the over coordination ($\Delta_i > 0$) and under coordination ($\Delta_i < 0$) energy, respectively. Over coordination (equation (2)) is the difference between the total bond order around the atom and the number of its bonding electrons.

$$\Delta_i = -Val_i + \sum_{j=1}^{neighbours(i)} BO_{ij} \quad (2)$$

where Val_i is the number of bonding electrons, BO'_{ij} is the bond order and Δ'_i is the over coordination. E_{val}, E_{pen} and E_{coa} are the Valence energy terms which represent the angle energy, penalty energy and three-body conjugation term, respectively. E_{tors} and E_{conj} are the torsion angle terms, which are the torsion rotation barriers and the four-body conjugation, respectively. E_{H-bond} is the hydrogen bond interaction, E_{C_2} is the correction for C_2 ,and E_{trip} is the triple bond energy correction. . $E_{vdWaals}$ and $E_{Coulomb}$ present the nonbonded interactions, van der Waals interactions and Coulomb.

In the next step, energy minimization is carried out at the beginning of the simulation by using Conjugate gradient algorithm [20–22]. For temperature control of the system Berendsen thermostat method [23] is used, which resets the temperature of atoms and rescale their velocity every time step. Since the temperature through this reaction is lower than 500 k, a time step of 0.5 fs is considered.

III. RESULTS AND DISCUSSION

Effects of the flow velocity and concentration of ethanol molecules on the adsorption process are studied, which includes sixteen different cases (Table II). Properties of aluminum, ethanol molecules and parameters considered in MD simulations are presented in Table I.

The total potential energy and total pressure of the system are good indicators of the steady state condition (Figure 2). The binding process becomes more complicated for cases with higher concentration and flow velocity and they would need more time to reach the steady state condition.

Radial distribution function (RDF) is used to study the surface properties (Equation 3). RDF presents the probability of finding a particle at a specific distance from another particle. In this work adsorption of oxygen atoms to Aluminum is set as the two targets, since oxygen is the leading atom in this adsorption process. RDF is calculated based on the distance between Oxygen and Aluminum atoms, using Equations (3) and (4) [24] .

$$\mathrm{g(r)} = \frac{1}{\rho 4\pi r^2 \delta\varepsilon} \frac{\sum_{t=1}^{\tau}\sum_{j=1}^{N} \Delta N\left(r \overset{\Delta}{\rightarrow} r + dr\right)}{N \times \tau} \quad (3)$$

$$\mathrm{g(r)} = \mathrm{c_{Al}^2 g_{Al-Al}(r)} + 2\mathrm{c_O c_{Al} g_{Al-O}(r)} + \mathrm{c_O^2 g_{O-O}(r)} \quad (4)$$

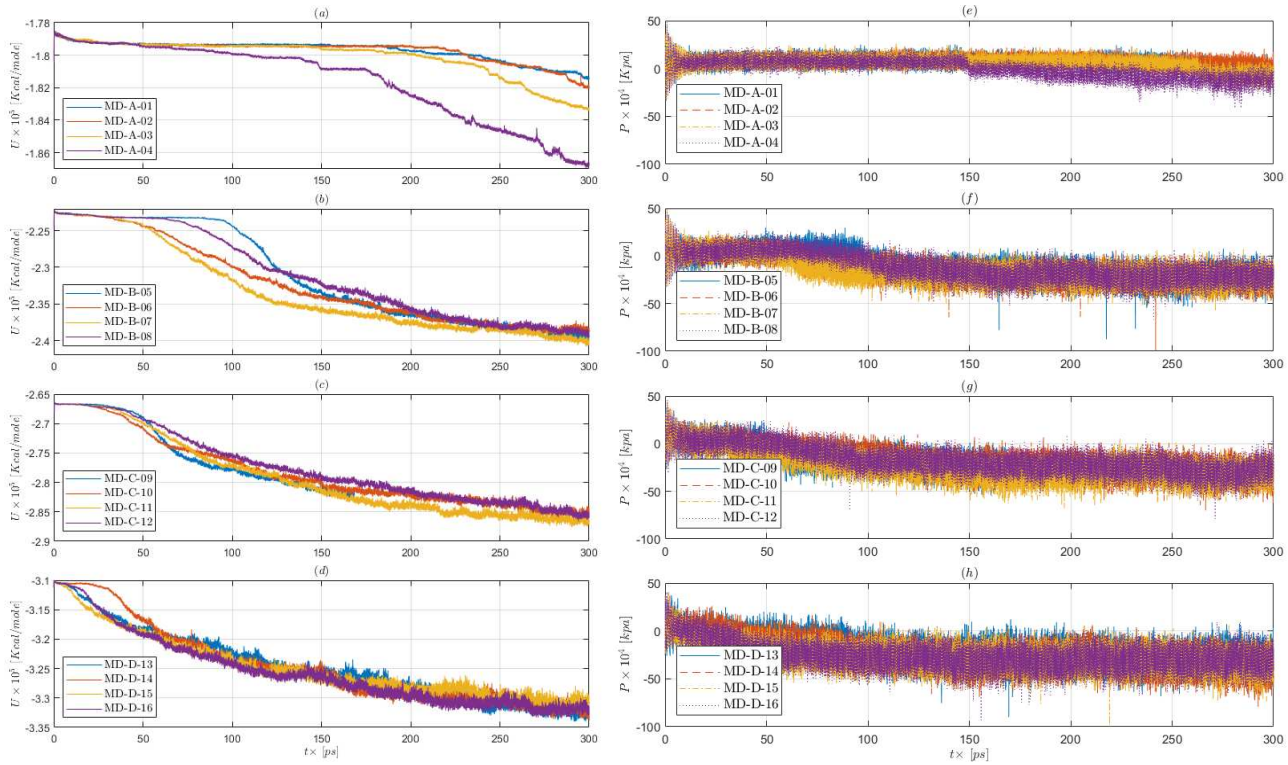

Figure 2. . Total energy of the system for different concentration of targeted molecules from low concentration to high concentration (50 (a), 100 (b), 150 (c) and 200 (d) ethanol molecules).Total pressure of the system for different concentration of targeted molecules from low concentration to high concentration (50 (e), 100 (f), 150 (g) and 200 (h) ethanol molecules).

where τ is the total computational time, r is the distance from the reference atom, N is the total number of atoms, c_{AL} is the concentration of Aluminium, c_O is the concentration of Oxygen in the system. The RDF peak at $1.8 \times 10^{-10} m$ is obtained for all cases, representing the Aluminum and Oxygen binding distance (Figure 3). The change in maximum RDF has a direct ratio with velocity, for the cases with lower concentration, although it is not relevant for cases MD-C and MD-D due to the suffusion of the surface (Table II). Increase of the velocity, further than $0.1\ \mathrm{m/s}$, does not have a significant effect on the total adsorbed targets at the end of the 300 ps (e.g., cases MD-A-03 and MD-A-04 in Figure 3-e). Adsorption of ethanol molecules on the sensor surface through time is presented in Figure 3-e. For series MD-A, as predicted, it has an increasing trend in adsorption by increase in velocity. Although this trend cannot be seen in the other series. This change is more evident through cases MD-A-02 and MD-A-03, where there is more than 80% increase in the number of adsorbed molecules.

IV. Conclusion

A molecular dynamics model is developed using the ReaxFF potential to study the effect of concentration and

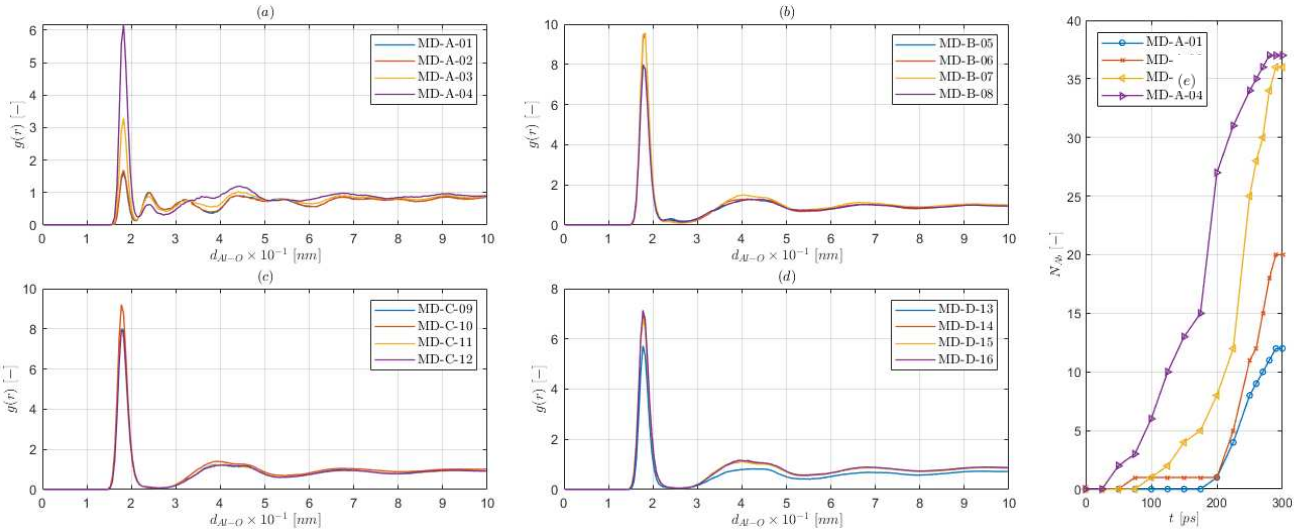

Figure 3. Radial distribution function (RDF) for different cases through time, in different velocities (from 0.001 m/s to 1m/s), for cases MD-A (a), MD-B (b), MD-C (c) and MD-D (d), respectively. Adsorption of ethanol on the sensor surface through time for series MD-A (e).

velocity on the binding process of an Aluminum-based biosensor.

TABLE II. THE DETAILS OF CASES MD-A, B, C AND D.

Details	*Velocity* (m/s)	$N_{tm}{}^{a}$	$g(r)_{max}$
MD-A-01	10^{-3}	50	1.61
MD-A-02	10^{-2}	50	1.69
MD-A-03	10^{-1}	50	3.29
MD-A-04	1	50	6.19
MD-B-05	10^{-3}	100	7.88
MD-B-06	10^{-2}	100	9.55
MD-B-07	10^{-1}	100	9.51
MD-B-08	1	100	7.98
MD-C-09	10^{-3}	150	8.03
MD-C-10	10^{-2}	150	9.21
MD-C-11	10^{-1}	150	8.03
MD-C-12	1	150	7.96
MD-D-13	10^{-3}	200	5.72
MD-D-14	10^{-2}	200	7.04
MD-D-15	10^{-1}	200	6.82
MD-D-16	1	200	7.15

a. Number of target molecules

This method has been validated using the quantum mechanics data from previous literature. Based on the results, increase in velocity can significantly decrease the adsorption time, as well as 7-80% increase in adsorbed target molecules, for the cases with less than 100 Ethanol molecules. For higher concentration cases, it is more challenging for the molecules to find free-binding sites. Hence, in the next step of this work, machine learning methods will be implemented to predict the full performance of the sensor and enhance the design process of bio sensing technologies.

ACKNOWLEDGMENT

The first author would like to thank the Department of MACE at the University of Manchester for providing Ph.D. funding under the "Exceptional Women in Engineering" scheme.

REFERENCES

[1] De Oliveira, R.A., Nicoliche, C.Y., Pasqualeti, A.M., Shimizu, F.M., Ribeiro, I.R., Melendez, M.E., Carvalho, A.L., Gobbi, A.L., Faria, R.C. and Lima, R.S., 2018. Low-cost and rapid-production microfluidic electrochemical double-layer capacitors for fast and sensitive breast cancer diagnosis. Analytical chemistry, 90(21), pp.12377-12384.

[2] Devi, M., 2020. Application of 2D Nanomaterials as Fluorescent Biosensors. In Adapting 2D Nanomaterials for Advanced Applications (pp. 117-141). American Chemical Society.

[3] Ruiz-Valdepeñas Montiel, V., Povedano, E., Vargas, E., Torrente-Rodríguez, R.M., Pedrero, M., Reviejo, A.J., Campuzano, S. and Pingarrón, J.M., 2018. Comparison of different strategies for the development of highly sensitive electrochemical nucleic acid biosensors using neither nanomaterials nor nucleic acid amplification. ACS sensors, 3(1), pp.211-221.

[4] Ambhorkar, P., Wang, Z., Ko, H., Lee, S., Koo, K.I., Kim, K. and Cho, D.I.D., 2018. Nanowire-based biosensors: from growth to applications. Micromachines, 9(12), p.679.

[5] Tagit, O. and Hildebrandt, N., 2017. Fluorescence sensing of circulating diagnostic biomarkers using molecular probes and nanoparticles. ACS sensors, 2(1), pp.31-45.

[6] Wang, L., Lou, Z. and Shen, G., 2020. 2D Nanomaterials with Hierarchical Architecture for Flexible Sensor Application. In Adapting 2D Nanomaterials for Advanced Applications (pp. 93-116). American Chemical Society.

[7] Yang, A. and Yan, F., 2020. Flexible electrochemical biosensors for health monitoring. ACS Applied Electronic Materials, 3(1), pp.53-67.

[8] Shahbazi, F., Jabbari, M., Esfahani, M.N. and Keshmiri, A., 2021. A computational simulation platform for designing real-time monitoring systems with application to COVID-19. Biosensors and Bioelectronics, 171, p.112716.

[9] Shahbazi, F., Jabbari, M., Esfahani, M.N. and Keshmiri, A., 2020. Numerical framework for simulating bio-species transport in microfluidic channels with application to antibody biosensors. MethodsX, 7, p.101132.

[10] Liu, P.; Liu, J.; Wang, M.; Yi, C.; Wang, W.; Shen, C.; Liu, P.; Liu, J.; Wang, M.; Åkesson, P.; Chenoweth, K.; Duin, A. C. T. Van; Goddard, W. A. Adsorption of Ethanol Molecules on the Al (1 1 1) Surface: A Molecular Dynamic Study. R. Soc. Open Sci. 2019, 6 (1), p.10.

[11] Li, Y., Liao, M. and Zhou, J., 2017. Catechol–cation adhesion on silica surfaces: molecular dynamics simulations. Physical Chemistry Chemical Physics, 19(43), pp.29222-29231.

[12] He, Z.; Zhou, J. Probing Carbon Nanotube-Amino Acid Interactions in Aqueous Solution with Molecular Dynamics Simulations. Carbon N. Y. 2014, 78, p.500–509.

[13] Su, L., Krim, J. and Brenner, D.W., 2018. Interdependent roles of electrostatics and surface functionalization on the adhesion strengths of nanodiamonds to gold in aqueous environments revealed by molecular dynamics simulations. The journal of physical chemistry letters, 9(15), pp.4396-4400.

[14] Pfrommer, B.G., Côté, M., Louie, S.G. and Cohen, M.L., 1997. Relaxation of crystals with the quasi-Newton method. Journal of Computational Physics, 131(1), pp.233-240.

[15] Van Duin, A. and Kimberly, C., 2001. ReaxFF Potential Functions. Journal of Physical Chemistry A, 2, pp.1-10.

[16] Liu, P., Liu, J. and Wang, M., 2019. Adsorption of ethanol molecules on the Al (1 1 1) surface: a molecular dynamic study. Royal Society open science, 6(1), p.181189.

[17] Van Duin, A., Verners, O. and Shin, Y.K., 2013. Reactive force fields: concepts of ReaxFF and applications to high-energy materials. International Journal of Energetic Materials and Chemical Propulsion, 12(2).

[18] Senftle, T.P., Hong, S., Islam, M.M., Kylasa, S.B., Zheng, Y., Shin, Y.K., Junkermeier, C., Engel-Herbert, R., Janik, M.J., Aktulga, H.M. and Verstraelen, T., 2016. The ReaxFF reactive force-field: development, applications and future directions. npj Computational Materials, 2(1), pp.1-14.

[19] Van Duin, A. and Kimberly, C., 2001. ReaxFF Potential Functions. Journal of Physical Chemistry A, 2, pp.1-10.

[20] Guénolé, J., Nöhring, W.G., Vaid, A., Houllé, F., Xie, Z., Prakash, A. and Bitzek, E., 2020. Assessment and optimization of the fast inertial relaxation engine (fire) for energy minimization in atomistic simulations and its implementation in lammps. Computational Materials Science, 175, p.109584.

[21] Bitzek, E., Koskinen, P., Gähler, F., Moseler, M. and Gumbsch, P., 2006. Structural relaxation made simple. Physical review letters, 97(17), p.170201.

[22] Sheppard, D., Terrell, R. and Henkelman, G., 2008. Optimization methods for finding minimum energy paths. The Journal of chemical physics, 128(13), p.134106.

[23] Berendsen, H.J.C. and Postma, J.P., 1984. M; DiNola, A.; Van Gunsteren, WF; Haak. J Chem Phys, 181, pp.3684-90.

[24] Sheybani, Z., Dokoohaki, M.H., Negahdaripour, M., Dehdashti, M., Zolghadr, H., Moghadami, M., Masoompour, S.M. and Zolghadr, A.R., 2020. The role of folic acid in the management of respiratory disease caused by COVID-19.

[25] Canalejas-Tejero, V., Herranz, S., Bellingham, A., Moreno-Bondi, M.C. and Barrios, C.A., 2014. Passivated aluminum nanohole arrays for label-free biosensing applications. ACS applied materials & interfaces, 6(2), pp.1005-1010.